Aerodynamic characterisation of green wall vegetation based on plant morphology : an experimental and computational fluid dynamics approach

Aerodynamic characterisation of green wall vegetation based on plant morphology: an experimental and computational fluid dynamics approach

Kyra Koch[a,*], Roeland Samson[a], Siegfried Denys[b]

[*]: corresponding author, e-mail: kyra.koch@uantwerpen.be, T: +32 3 265 35 69
[a]: Research group ENdEMIC, Department of Bioscience Engineering, University of Antwerp, Groenenborgerlaan 171 2020 Antwerp, Belgium
[b]: Research group DuEL, Department of Bioscience Engineering, University of Antwerp, Groenenborgerlaan 171 2020 Antwerp, Belgium

Abstract

The installation of urban green infrastructure, particularly green walls, has proven to be an effective strategy for the mitigation of particulate matter (PM) pollution and the urban heat island effect. For the interaction between vegetation, PM and the local microclimate, wind flow is the main driving force. In order to investigate these interactions in detail, it is important to know how air flows through vegetation. This study proposes a method based on the Darcy-Forchheimer equation, where vegetation is considered as a porous medium and several plant species and the effects of plant morphological characteristics are examined both experimentally and using computer simulations. Results showed that the Darcy-Forchheimer model is a simple and robust way to describe air flow through vegetation regardless of its morphology. This research provides a new vision on studying aerodynamic properties of vegetation in relation to their morphology and provides opportunities for modelling the interaction between vegetation and its environment.

Keywords: Darcy-Forchheimer; CFD; wind tunnel; air flow; vegetation morphology

Nomenclature table

A	Area	m^2
FLS	Functional leaf size	(-)
K	Permeability	m^2
K_1	Inertial permeability	m
LAD	Leaf area density	$m^2\ m^{-3}$
LDI	Leaf dissection index	(-)
LS	Leaf size	m^2
LSS	Leaf surface structure	(-)
LR	Leaf ratio	(-)
M	Mass	kg
P	Perimeter	m
PAD	Plant area density	$m^2\ m^{-3}$
Q	Flow rate	$m^3\ s^{-1}$
R^2	Coefficient of determination	(-)
SLA	Specific leaf area	$m^2\ kg^{-1}$
q	Flux	$m\ s^{-1}$
v	Fluid velocity	$m\ s^{-1}$
V	Volume	m^3
ΔP	Pressure loss	Pa
ΔP_{norm}	Normalised pressure loss	(-)
Δx	Distance	m
ρ	Density	$kg\ m^{-3}$
φ	Porosity	(-)
τ	Kendall rank correlation coefficient	(-)
μ	Viscosity	Pa s

1 Introduction

Over the last decade green walls and façades have become an increasingly popular type of urban green infrastructure (UGI). They provide an efficient way to introduce green environments in the limited space typically available in the urban environment provided they are thoughtfully planned (Cameron & Blanuša, 2016). UGI is able to fulfil many different ecosystem services (ES), including air quality improvement (by particulate matter [PM] deposition) (Abhijith et al., 2017; Gallagher et al., 2015), environmental cooling, carbon sequestration, increasing biodiversity and also serving social and cultural purposes (Madre, Clergeau, Machon, & Vergnes, 2015; Tallis et al., 2015; White & Gatersleben, 2011). Improvements in air quality and environmental cooling are significantly driven by physical interactions between the plants and air flowing over and through them. Vegetation affects local air flow and it therefore alters wind-driven processes such as PM deposition (K. P. Beckett, Freer-Smith, & Taylor, 1998; Janhäll 2015; Litschike & Kuttler, 2008; Nowak, Crane, & Stevens, 2006; Ottelé, van Bohemen, & Fraaij, 2010; Pugh, Mackenzie, Whyatt, & Hewitt, 2012; Tallis et al., 2015), evaporation and heat transfer (Demuzere et al., 2014; Hunter et al., 2014; Perini, Ottelé, Fraaij, Haas, & Raiteri, 2011; Tallis et al., 2015).

Several investigations have demonstrated the influence of vegetation on local air flow, based either on field measurements (Hong, Lin, Wang, & Li, 2012) or wind tunnel studies using plant imitators (Buccolieri, Gromke, Di Sabatino, & Ruck, 2009; Endalew et al., 2009; Gromke 2011 and references therein; Gromke et al., 2016) or real plants (Molina-Aiz, Valera, Álvarez, & Madueño, 2006; Lin & Khlystov, 2012a; Sase, Kacira, Boulard, & Okushima, 2012). Some studies were based on numerical airflow models (Connell, Endalew, & Verboven, 2011; De Maerschalck, Maiheu, Janssen, & Vankerkom, 2010; Endalew et al., 2009; Hong et al., 2012) or empirical models (Raupach, Woods, Dorr, Leys, & Cleugh, 2001; Tiwary, Morvan, & Colls, 2005; M. Lin, Katul, & Khlystov, 2012b) or a combination of multiple approaches. Most model-based studies considered vegetation as rigid structures, omitting realistic descriptions of micro-scale parameters, such as porosity and leaf morphology *within* vegetation stands. This simplification of the vegetation structure increases the uncertainty in study outputs. Moreover, few studies have been performed on the dynamics of air flowing *through* vegetation. This knowledge gap can be explained by the complexity of a vegetation stand and the physics involved, with randomly distributed air spaces between inhomogeneous foliage elements, causing flows with high turbulence (Tiwary et al., 2005). Also, drag forces may affect the airflow. The aerodynamic effects of plant stands are often expressed in terms of resistance to the flow or a drag coefficient (Molina-Aiz et al., 2006; Sase, Kacira, Boulard, & Okushima, 2012). Endalew et al. (2009) modelled the interaction between airflow and vegetation based on leaf drag/area and volume weighted drag (based on porosity), but for both methods detailed 3D geometrical information is needed (Endalew et al., 2009 and references therein). However, given the complexity of the systems under study, some simplification is recommended when modelling the dynamics of air flowing through vegetation.

This paper proposes a method based on the Darcy-Forchheimer equation (Nield, 2000). This equation originates from earth sciences where it is used to describe the flow of water through porous soils, but it has been proven to be applicable in many more research fields involving fluid flow (including air) through porous media (Bartzanas, Kittas, & Boulard, 2002; Bartzanas, Katsoulas, & Kittas, 2012; Mattis, Dawson, Kees, & Farthing, 2012a; Miguel, van de Braak, & Bot, 1997; Verbruggen et al., 2016). The Darcy-Forchheimer equation is an extension of the simple Darcy equation that relates the pressure drop observed when a fluid flows through a porous medium to the flow rate of the fluid. The Forchheimer-drag includes inertial effects that occur at high flow rates. Molina-Aiz et al., (2006) found that, when air

velocity and pressure drop are plotted, the Darcy-Forchheimer equation seemed to have the best fit with their wind tunnel data compared to drag equations.

The objectives of this study are (1) to assess whether the Darcy-Forchheimer equation is applicable to describe air flow through vegetation; (2) to investigate whether there are significant differences in the corresponding aerodynamic parameters between plant species and if so, (3) to check whether aerodynamic parameters can be related to plant species morphology.

2 Materials and methods

2.1 Selection of species and morphology

In order to cover the high variability in morphology typical for green wall vegetation, a broad range of plant species were selected according to their occurrence in green walls. Climbers/creepers as well as herbaceous species were chosen to cover both soil-bound and substrate-bound vertical garden systems, and a broad range in leaf morphological characteristics, like e.g. leaf size and shape (Table 1).

Table 1: Selected species and their morphological characteristics. Scientific name, leaf shape and length and width of an individual leaf are given.

Scientific name	Leaf morphology	Length x width	Scientific name	Leaf morphology	Length x width	Scientific name	Leaf morphology	Length x width
Hedera helix	Heart shaped	70 x 100 mm	*Campanula isophylla*	Heart shaped, serrated	40 x 45 mm	*Lonicera nitida*	Oval	15 x 5 mm
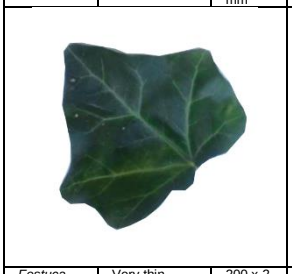						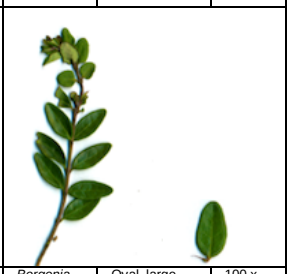		
Festuca glauca	Very thin grass	200 x 2 mm	*Fragaria sp.*'Ostara'	Ternate leaf, leaflets serrated	120 x 120 m0m	*Bergenia cordifolia*	Oval, large, thick	100 x 200 mm
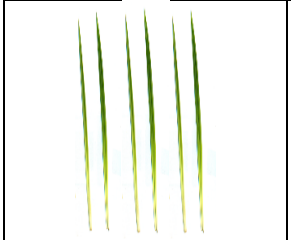								
Geranium traversii × *oxonianum*	Hand shaped, lobed	50 x 60 mm						
								

A series of directly measurable morphological plant parameters was examined. Morphological parameter selection was based on their potential to affect the air flow through vegetation. Each of these parameters is able to explain some aspects of leaf morphology into a single metric, which makes inter-

species comparison possible. An overview is given in Table 2. Methods were original unless stated otherwise with a reference.

Plant area density (PAD) is the amount of one sided plant surface (including twigs; A_{plant}) per total bulk volume (the volume of the cylinder holding the plants) (V_{total}) and a measure of how vegetation can fill up a space. It is closely related to porosity which is the void volume fraction of a porous material (see further). Plant surface was measured with a Li-3100c leaf area meter (Li-cor Inc., Lincoln, NE, USA). PAD is similar to *leaf area density* (LAD), which is more commonly used in plant ecology and considers only the one sided leaf surface. However, because in this study species with a highly diverse morphology were used and branches also affect local air flow, PAD is a better choice, as it is the total portion of plant material which contributes to pressure losses. Realistic PAD values were pursued without omitting extremely sparse or dense vegetation.

Volumetric *porosity* (φ) is the void volume fraction ($1-[V_{plant}\ V_{total}^{-1}]$) of a porous material. In this context, it is the volume fraction occupied by the air filled spaces in between the leaves and branches of the vegetation, and is typically higher than 93% (Gromke, Buccolieri, Di Sabatino, & Ruck, 2008). It should not to be confused with the 'optical porosity', which is a two-dimensional parameter that ignores some spatial information. Plant volume was determined through displacement by putting the vegetation in a graduated cylinder filled with water. Despite being the best empirical method to estimate the volume of an irregular shaped object, this method is quite crude. Therefore, as a quality control for each species, the volume was correlated with dry mass.

The *leaf ratio* (LR) is the amount of leaf material with respect to the total amount of plant material, calculated both in mass or volume units. The mass based leaf ratio was assessed by weighing leaves and stems that were dried in an oven (Memmert UF 260, Memmert, Eeklo, Belgium) separately on an analytical balance (S-234, Denver Instruments, NY, USA, accuracy= 0.1 mg). These masses were averaged for every species, with between 8 and 15 replicates per species, and the correlation between weight and volume based leaf ratios was identified.

Specific leaf area (SLA) (Cornelissen et al., 2003) is expressed as the one-sided leaf surface (A_{leaf}) with respect to leaf dry mass (M_{leaf}). Dry matter was measured on the analytical balance (accuracy = 0.1 mg). This parameter can be used as a measure for leaf structure/thickness (Vile et al., 2005). One average SLA value was calculated for every species out of 8 to 15 replicates. Including mass in a dataset can be beneficial, as most other parameters only cover a two dimensional representation of vegetation, while mass is also indicative for the occupied volume.

Leaf dissection index (LDI) can be described as the ratio of a leaf's perimeter (P_{leaf}) to the square root of its surface area ($\sqrt{A_{leaf}}$) (McLellan & Endler, 1998). This is a dimensionless parameter which is used to describe leaf shape. Plant species that have strongly incised or elongated leaves have a higher LDI than plants which have leaves with a more circular shape. The minimum value for LDI is 3.545, this is the value for a perfect circle. The square root of leaf area is taken in order to normalize for leaf size, as the test plants had leaves with similar shapes but different sizes. LDI was determined for every species by measuring six undamaged leaves over their leaf size range, of which the mean value was taken as the species' LDI. It should be noted that for *Fragaria* sp. only one leaflet was considered, as one full leaf consist of three fully separated petioles.

Functional leaf size (FLS) is the surface of the largest full circle that can be drawn into a leaf (A_{circle}), normalized by leaf surface (A_{leaf}). This parameter is the major determinant of the leaf boundary layer

and thus strongly influences PM deposition and transpiration. Per species one value for FLS was retrieved by taking the mean of six leaves of varying sizes as used for LDI. For species of which the leaves were consisting of multiple leaflets (e.g. *Fragaria* sp.), again only the single leaflet was considered.

Leaf size (LS) is the one-sided surface area of a leaf (A_{leaf}). Per species one value for leaf size was taken as an average from six individual undamaged leaves over their size range.

Leaf surface structure (LSS) was assessed by categorization. Hairy leaves and leaves with rough (irregular) surfaces, at microscopic level, are known to sustain a thicker boundary layer than non-hairy and smooth leaves. This could have an influence on local air flow (turbulence), PM deposition and gas exchange processes. Of each species, SEM (scanning electron microscope) images were taken with a Quanta FEG 250 at high vacuum. For full explanation of the methodology we refer to Castanheiro, Samson, & De Wael (2016). Surface characteristics were divided into 3 categories and categorized as very hairy and/or irregular (considered as '2'), semi-hairy and/or semi-irregular ('1'), and smooth ('0').

For LR, SLA, LDI, FLS and LS results are presented as mean values with a standard deviation.

Table 2: Overview of determined plant morphological parameters. V: volume (m^3), A: leaf surface (m^2), P: leaf perimeter (m), M: dry leaf mass (kg)

Parameter	Formula	Unit
Plant Area Density (PAD)	$PAD = \frac{A_{plant}}{V_{total}}$	$m^2\ m^{-3}$
Porosity (ϕ)	$\varphi = 1 - \left(\frac{V_{plant}}{V_{total}}\right)$	dimensionless
Leaf Ratio (LR)	*LR = 1 – stem ratio*	percentage
Specific Leaf Area (SLA)	$SLA = \frac{A_{leaf}}{M_{leaf}}$	$m^2\ kg^{-1}$
Leaf Dissection Index (LDI)	$LDI = \frac{P_{leaf}}{\sqrt{A_{leaf}}}$	dimensionless
Functional Leaf Size (FLS)	$FLS = \frac{A_{circle}}{A_{leaf}}$	dimensionless
Leaf size (LS)	A_{leaf}	m^2
Leaf Surface Structure (LSS)		

2.2 Experimental procedure

2.2.1 Wind tunnel experiments

Pressure losses over vegetation were measured in a continuous flow, closed circuit wind tunnel (Fig. 1 left). The circuit consists of circular air ducts (inner diameter 103 mm) with a total length of 6 m. A plant compartment consisting of a transparent pipe (length 545 mm, inner diameter 114 mm) was fitted in the closed circuit. Air movement was created by a continuously controllable inline duct fan which could induce wind speeds varying from 1.14 to 4.40 m s^{-1} (for an empty compartment), which is a realistic but low range of wind speeds. Air velocity induced by the duct fan was measured by a hotwire air velocity sensor (CTV 110, KIMO Instruments, Chevry-Cossigny, France). Instead of continuously varying the airflow rate during an experiment, the power supply to the duct fan was controlled and fixed at five power supply settings: the minimum and maximum power supply (corresponding to the minimum (but

not zero) and maximum wind speed), and approximately the 1st, 2nd (median) and 3th quartile. The advantage of selecting five specific power supplies was that for each setting, a corresponding fan curve (i.e. the relation between the pressure loss and the flow rate for the fan used) could be determined from all pressure loss and velocity measurements (for all species under study) corresponding to the specific power supply. The fan curves could then be used as boundary conditions in the models (see further). Obviously, the air velocity *v* is not uniform over the cross section of the flow. Mostly, average velocities are used in the analysis of duct flow. Air velocity profiles were derived from measurements with the hot wire velocity sensor located at different distances from the duct wall and the average air velocity was calculated by integrating the profile over the flow cross section.

Freshly cut plant specimens were brought into the plant compartment of the wind tunnel and stacked as homogeneously as possible with the least possible clustering (Fig. 1 right), approximating the composition of the plants in a real green wall. After selecting one of the five power supply settings (always from low to high), the inline duct was switched on and the system was allowed to equilibrate until the pressure loss was stationary. Pressure loss (ΔP) over the plant compartment was assessed by a Pressure Module (750PD2, FLUKE Corporation, Gent, Belgium) with a range of ± 7 kPa and a Pressure Calibrator (717 30G, FLUKE Corporation). Test experiments showed similar results for the same vegetation specimen if brought multiple times into the wind tunnel in different configurations, providing that stacking was done uniformly. Only when heavily clustered, resulting in an inhomogeneous distribution within the plant compartment, did the results differ from each other. Therefore, each specimen was only tested once for a particular PAD under different airflow rates. Nevertheless, each plant species was tested at different PADs (Fig. 2 top) and porosities (Fig. 2 bottom) by adding or removing a certain amount of plant material. Vegetation was held in place by two grates, whose pressure loss was measured in a separate run in order to subtract the values from the vegetation measurements. Runs through an empty tunnel were used as a reference.

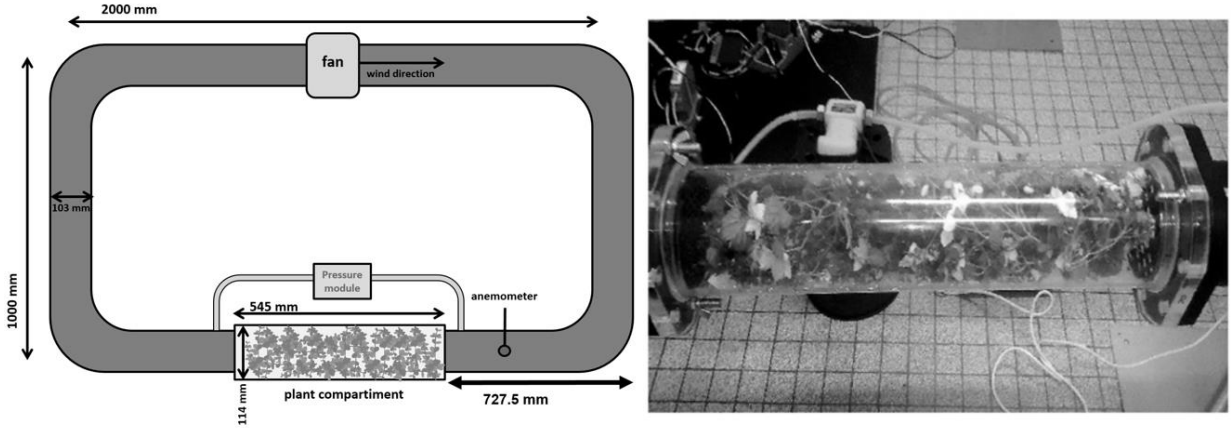

Fig. 1: Left panel: setup of the wind tunnel with the plant compartment filled with vegetation, right panel: plant compartment filled with fresh *Campanula* sp.

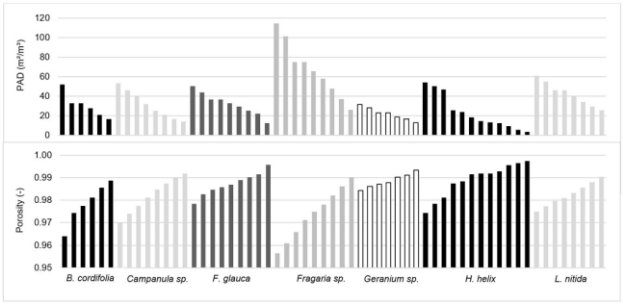

Fig. 2: PAD values for each run (top) and porosity values for each run (bottom). Species are sorted alphabetically.

2.2.2 Aerodynamic characterisation

In recent literature, an explicit approach is advised to simulate wind flow in urban areas where vegetation is present (Buccolieri et al., 2018). In most computation fluid dynamics (CFD) studies vegetation is considered as a porous medium, and additional terms are added to the momentum and turbulence equations to account for the loss of energy (refs from Buccolieri et al., 2018). While most published work focused on aerodynamic effects in the vicinity of trees, a characterisation of the air flow through vegetation was performed, and parameterised in a CFD model by adding pressure loss terms described in terms of permeability (for viscous losses) and 'inertial permeability' (for inertial losses). Since the intention was to correlate plant morphological parameters to aerodynamic parameters, a limited set of aerodynamic parameters was needed.

From pressure loss measurements over the plant compartment stacked with vegetation, it is possible to calculate the permeability of the vegetation to fluid flow. The permeability of a porous material is its ability to allow a fluid to pass through it and is closely related to its structure and porosity. For vegetation, which always has high values for porosity (often over 95%), leaf size and morphology were expected to be the determining parameters. At low fluid velocities (Reynolds numbers up to 10), the permeability of a porous material (K) can be simply derived from Darcy's law as:

$$K = \frac{v\ A\ \mu\ \Delta x}{\Delta P} \quad \text{(Eq. 1)}$$

where v is the bulk fluid speed (m s^{-1}) (the mean speed within the pores of the porous media), μ the viscosity of the fluid (Pa s), Δx the length of the porous medium (m), A the cross section area of the flow (m^2) and ΔP the pressure loss (Pa). The simple Darcy equation assumes a linear relation of fluid flow rate (or velocity) and pressure loss, and a unique value for the permeability. However, for very high velocities (Reynolds numbers being multitudes of 10) in porous media, inertial effects become important and an inertial quadratic term, known as Forchheimer-drag, needs to be added to the Darcy equation. This term accounts for the kinetic energy and inertia of the fluid and the typical non-linear relation of fluid flow rate and the pressure drop (S. A. Mattis, Dawson, Kees, & Farthing, 2012b):

$$\frac{\Delta P}{\Delta x} = -\left(\frac{\mu}{K}\right) q - \left(\frac{\rho}{K_1}\right) q^2 \quad \text{(Eq. 2)}$$

where K_1 is the inertial permeability (m), ρ the fluid density (kg m^{-3}) and q the fluid flux (m s^{-1}), calculated as:

$$q = v\ \varphi \quad \text{(Eq. 3)}$$

where φ represents the porosity (-). The term $\frac{\rho}{K_1}$ is called the Forchheimer-drag coefficient. Notice that in all calculations, the average air velocity (see section 3.2) was used.

For each of the species, the pressure loss was measured as a function of average air velocity. The permeability (K) and Forchheimer-drag ($\frac{\rho}{K_1}$) were obtained by regression of Eq. 2. Obviously, the amount of plant material brought in the compartment affects the PAD, the porosity and the aerodynamic parameters. Experiments were repeated with 8 to 15 different PAD's per species, depending on how easily the vegetation could be stacked and how long the branches stayed fresh (see Fig. 2). A wind tunnel experiment for one species took approximately one day. This was no problem with species such as Hedera, but more sensitive species, for example Fragaria became weak towards the end of the experiment so fewer wind tunnel tests could be performed.

In some cases, regression led to negative values for permeability and/or inertial permeability. This was solved by modifying the polynomial (Eq. 2) to a linear equation as follows:

$$\frac{\Delta P}{\Delta x\ q} = -\left(\frac{\mu}{K}\right) - \left(\frac{\rho}{K_1}\right) q \qquad \text{(Eq. 4)}$$

K and $\frac{\rho}{K_1}$ could then be retrieved by simple linear regression. Samples for which parameters remained negative were left out, as these physical impossible outcomes were attributed to flaws in those particular runs. In order to compare the aerodynamic characteristics of different species under similar conditions of wind velocity and PAD, pressure losses were normalised for wind velocity and PAD, so that a dimensionless, normalized pressure loss (ΔP_{norm}) can be defined as:

$$\Delta P_{norm} = \frac{\Delta P}{\rho\ v^2\ PAD\ \Delta x} \qquad \text{(Eq. 5)}$$

where $\rho\ v^2$ is a measure of kinetic energy per unit volume, also called dynamic pressure (Pa).

2.2.3 Calculations and statistical analysis

All calculations and analysis were performed in R version 3.3.1 (https://cran.r-project.org/) and an Excel spreadsheet. Within species morphological parameters, significant differences are identified with a Tukey-HSD test and these differences are indicated with the letters A, B and C. Due to the nature of the permeability and Forchheimer-drag data we performed a log (ln) transformation for normalization. Herewith an ANOVA was executed for looking at the variance between permeability and Forchheimer-drag between species. A Tukey-HSD test was performed to see where the differences are between species. A Kendall rank correlation test was performed for testing differences between permeability and Forchheimer-drag against porosity and PAD. A Kendall rank correlation test is comparable to a Spearman's test but stronger and more robust considering outliers as our data is highly skewed. Larger tau-values (always between 0 and 1) mean stronger correlations. Finally, to explain variance in permeability and Forchheimer-drag, linear models of the mean and median of permeability and Forchheimer-drag against SLA, LDI, FLS, LR, LS and LSS were made.

2.3 Numerical modelling

To test whether the aerodynamic parameters derived from the wind tunnel experiments can be used in a modelling approach, a numerical model of the wind tunnel was developed. The advantage of a numerical modelling approach such as CFD is that geometrical effects (realistic green walls with complex geometries) as well as (dynamic) climate boundary conditions can be tested. CFD simulations were conducted using the commercially available software package COMSOL Multiphysics® version 5.2a (COMSOL Inc., MA, USA). The geometry consisted of the entire wind tunnel (Fig. 3) including the plant compartment (which is slightly wider than the other ducts). Considering the symmetry of the geometry, only half of the geometry was meshed as shown in the figure. The computational grid consisted of approximately 170,000 tetrahedral cells with a boundary layer at the duct walls. Grid size independency was ensured by gradually refining the mesh until further refinement did not affect the results. The average mesh quality of the geometry was 0.72. Mesh quality is a compound quantity representing some quality attributes of the mesh elements (skewness, volume versus circumradius, growth rate, …). A quality of 1 indicates the best possible fit and an optimal element. At the other end of the interval, 0 represents a degenerated element. Under the flow rate conditions, a turbulent flow regime is expected and a k-ω turbulent, incompressible flow model at standard conditions (101325 Pa, 293.15 K) was considered in the ducts. In contrast to the laminar flow model, the k-ω model solves for extra variables: the turbulence kinetic energy and the rate of dissipation of turbulence kinetic energy ω. A steady-state solution was generated with a direct stationary solver (relative tolerance 0.001), by solving the governing equations of momentum and mass continuity in the wind tunnel ducts (Comsol 2017):

$$\rho(\mathbf{u}\cdot\nabla)\mathbf{u} = \nabla\cdot\left(-\mathrm{P}\mathbf{I} + (\mu+\mu_T)(\nabla\mathbf{u} + (\nabla\mathbf{u})^{\boldsymbol{T}})\right)$$

$$\rho\nabla(\mathbf{u}) = \mathbf{0}$$

With ρ the air density (1.2044 kg m^{-3}), $\mathbf{u}$ the velocity vector (m s^{-1}), $\mathbf{I}$ an identity matrix, P the pressure (Pa), μ the dynamic viscosity (Pa s) and μ_T the eddy viscosity (Pa s), which is calculated by the k-ω model for a turbulent flow and equals zero in the case of a laminar flow. Second order discretisation was set by default in all equations. In the plant compartment the air velocity and pressure fields were modelled using the Darcy–Forchheimer equation (Eq. 2), which considers single-phase flow in a porous medium. To couple the physics, the pressures at the boundaries between the air ducts (turbulent flow) and the plant compartment (Darcy-Forchheimer) were equalised. This is a convenient and computationally profitable approximation for single phase fluid flow in a porous medium (Bejan, 2013). For the duct walls a no-slip condition is used which means that the fluid velocity adjacent to the wall is zero. Wall roughness was chosen to be generic with standard roughness height and roughness parameter. The inline duct fan was modelled as an 'interior fan'. This boundary condition considers the static pressure curve data (the fan curve) of the actual duct fan. For the fan used in this study, five pressure/flow rate curves were determined corresponding to the five different power supply settings. Due to the different densities in plant material during the experiment, a trend line could be fitted through the data points on the pressure loss versus flow rate curve. This means that the more plant material that is present, the higher the pressure loss between the front and rear of the vegetation sample and the lower the air flowrate. Curves are at various positions for each chosen wind speed; at higher wind speeds there is a shift towards higher values. However, this relationship retains the same slope. The advantage of using the fan boundary condition is, that the model automatically finds the working point of the fan, corresponding to the

pressure losses imposed by the vegetation and all duct walls. Consequently, the velocity measured by the hot wire anemometer in the experiment can be used to validate the accuracy of the model, by plotting experimental and modelled values against each other. The same applies to the pressure loss measured by the pressure module and the modelled pressure loss. Permeability, porosity and Forchheimer-drag datasets were provided by the wind tunnel experiments. Apart from Darcy-Forchheimer, a simple Darcy model was tested as well. Model results for all experiments were obtained using a parametric sweep, which is the easiest way to find the solution for a sequence of input parameters. The mesh of the plant compartment was built at a larger element size, as a finer mesh would take too much computational time and computer capacity. The pressure losses, obtained by the model, were then compared with the experimentally measured values to test the method. As a validation, the modelled velocity was compared to the value measured by the anemometer, at the corresponding measuring point.

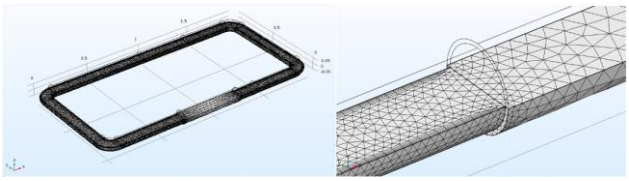

Fig. 3: Geometry of the wind tunnel (left) and the computational mesh used in the model (right)

3 Results

3.1 Species morphology

A series of species morphological parameters was determined in order to explain potential variance in pressure and permeability data. Fig. 4 on the left shows the mean LR per species. For *Campanula* (26% ± 0.04) the stem volume overrules the leaf volume. For *Geranium* (49% ± 0.01) and *Hedera* (50% ± 0.06), the ratio is 50/50. *Lonicera* (68% ± 0.01) and *Fragaria* (82% ± 0.06) possess more leaf than stem material in terms of volume. *Bergenia* (rozet plant) and *Festuca* (grass) both consist solely of leaves. LS (Fig. 4 right panel) shows *Bergenia* (741.2 mm^2 ± 421.3) to have the largest leaves, followed by *Fragaria* (335.5 mm^2 ± 236.6) and *Hedera* (288.4 mm^2 ± 265.4) which are close together. *Geranium* has small leaves (118.2 mm^2 ± 62.9) followed by *Campanula* (47.6 mm^2 ± 27.8). *Festuca* is a very fine grass (29.6 mm^2 ± 3.0) and *Lonicera* has the smallest leaves (11.1 mm^2 ± 6.6). SLA varied from 20.60 $m^2\ kg^{-1}$ ± 1.99 for *Fragaria*, down to 5.60 $m^2\ kg^{-1}$ ± 1.31 for *Hedera* (Fig. 5). Furthermore, FLS varied from 8.87×10^{-1} ± 0.08 for *Fragaria* down to 3.22×10^{-3} ± 0.001 for *Festuca* (Fig. 5). LDI of the species varied from 4.16 ± 0.3 for *Lonicera*, which has the roundest leaves to 33.8 ± 2.5 for *Festuca*, which is a grass. LSS varied widely between species, which made comparison complicated. Hence, surface structure was categorised into robust classes (Table 3). Based on an ANOVA-analysis no statistically significant correlations could be found between the species' morphological parameters.

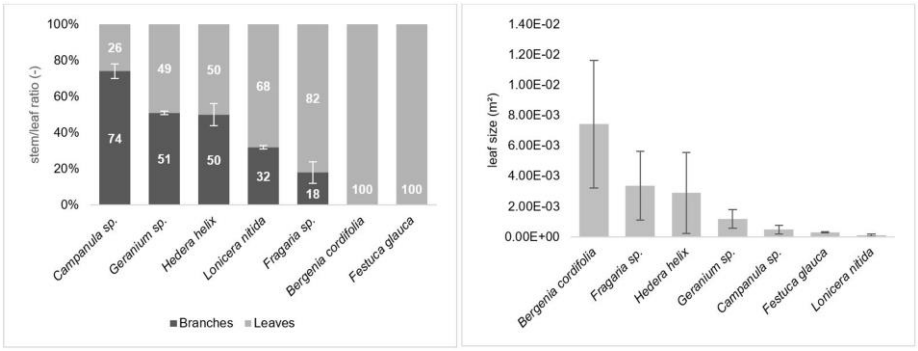

Fig. 4: Volumetric leaf ratio (LR) of the considered plant species, classified from lowest to highest

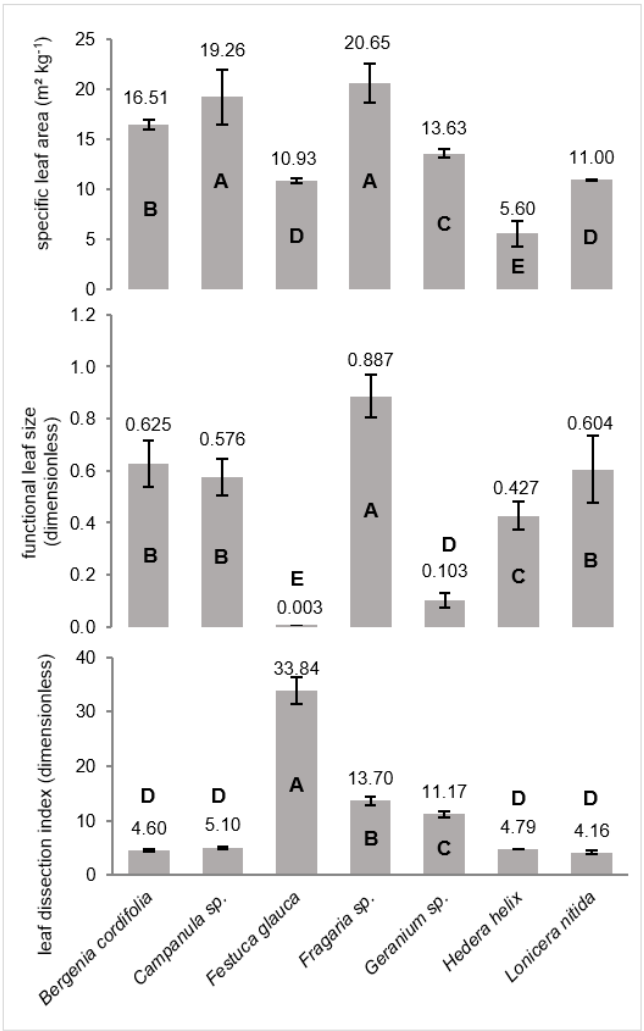

Fig. 5 (from top to bottom): Mean Specific Leaf Area (SLA), Functional Leaf Size (FLS) and Leaf Dissection Index (LDI) with standard deviations for all species, classified alphabetically according to species name. Different letters indicate significant differences.

Table 3: Leaf surface structure (LSS) divided into 3 categories: very hairy and/or irregular, semi-hairy and/or irregular, and smooth. Images were taken at 10 µm to 1 mm, depending on the size of the structures showed.

Very hairy and/or irregular	
Campanula sp. (1 mm)	*Fragaria sp.* (100 µm)
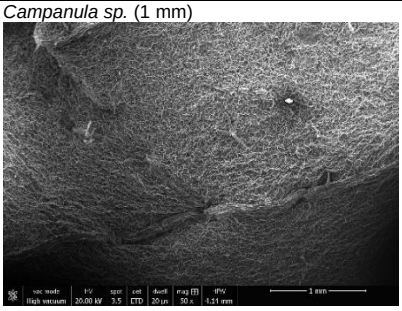	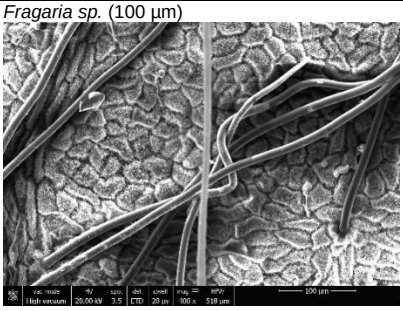
Geranium sp. (500 µm)	
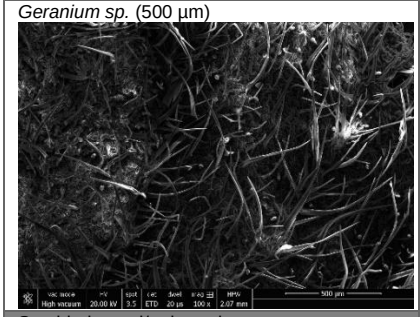	
Semi-hairy and/or irregular	
Hedera helix (1 mm)	*Festuca glauca* (50 µm)
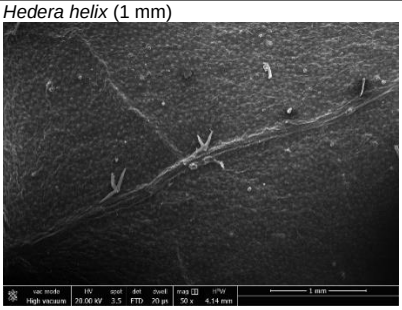	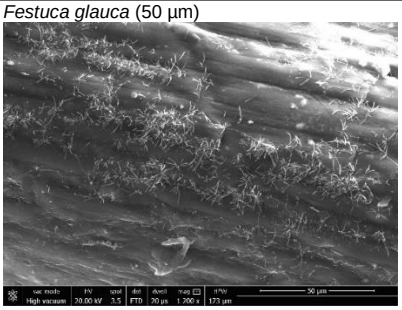
Smooth	
Lonicera nitida (300 µm)	*Bergenia cordifolia* (500 µm)
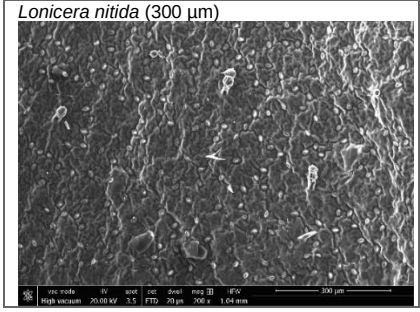	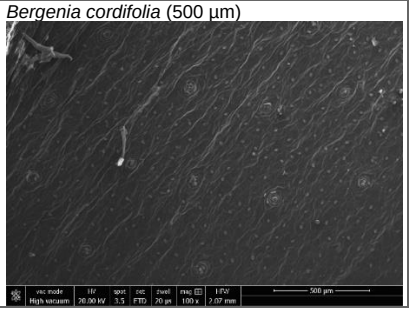

3.2 Aerodynamic characterization using wind tunnel experiments

Figure 6 shows the shape of the air velocity profiles, derived from measurements at the five power supply settings and three different positions in the tunnel duct (centre, 0.025 and 0.05 m from the centre). During the pressure loss experiments, air velocity was only measured in the centre of the duct and the average velocity was calculated by integration over the cross section surface of the duct, according to the profiles in Fig. 6. For further determination of the aerodynamic parameters, the average

velocity was used in the equations. Reynolds numbers were calculated for each run using the kinematic viscosity of air at 20° C which is 1.51×10^{-5} m^2 s^{-1}. Reynolds numbers varied from 2.33×10^4 to 1.50×10^5. These values indicate turbulent air flow, which justifies the use of Darcy-Forchheimer for further calculations.

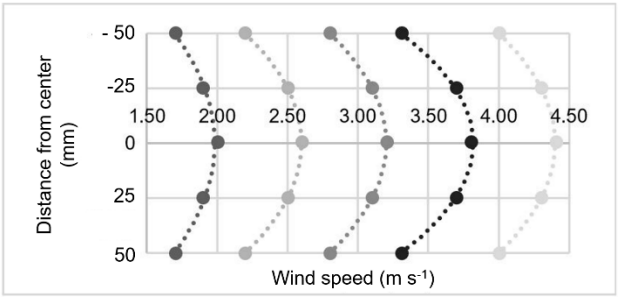

Fig. 6: Air velocity profiles at the five used power supply settings and three different positions in the tunnel duct (centre, 0.025 and 0.05 m from the centre). The dotted lines indicate polynomials plotted through the data points.

From the pressure loss measurements at a range of average air velocities, the permeability (K) and Forchheimer-drag (ρ/K_1) were obtained by regression using Eq. (2). Values of permeability and Forchheimer-drag varied from 1.59×10^{-7} m^2 to 4.71×10^{-5} m^2 and 5.09×10^{-1} kg m^{-4} to 7.80×10^{-1} kg m^{-4}, respectively. Data distribution for both permeability and Forchheimer-drag is heavily skewed. Therefore, to investigate the difference between species, a natural log transformation was performed. Normality could be confirmed by a Shapiro-Wilk normality test. Figure 7 shows differences in permeability (top) and Forchheimer-drag (bottom) between species. An ANOVA proved that log (K) is different between species ($p = 1.63 \times 10^{-5}$). The TukeyHSD test indicated where the differences are between species (A and B). On the other hand, log (ρ/K_1) did not differ between the species ($p = 0.09$).

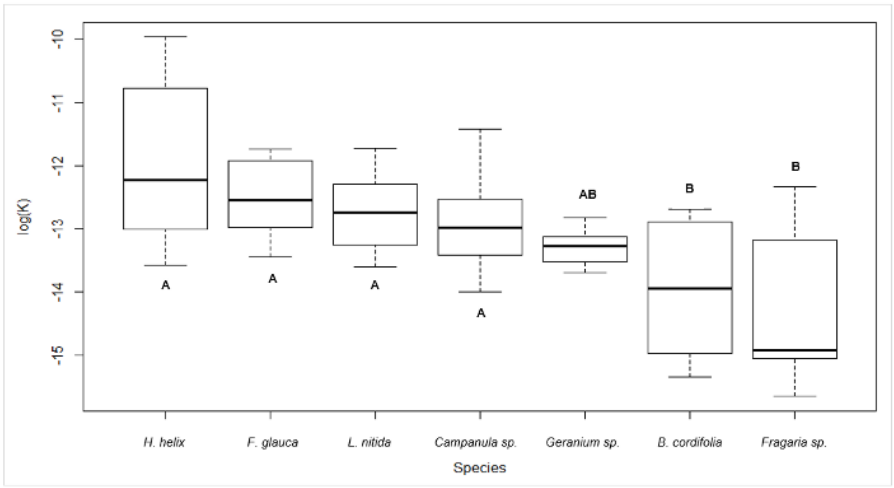

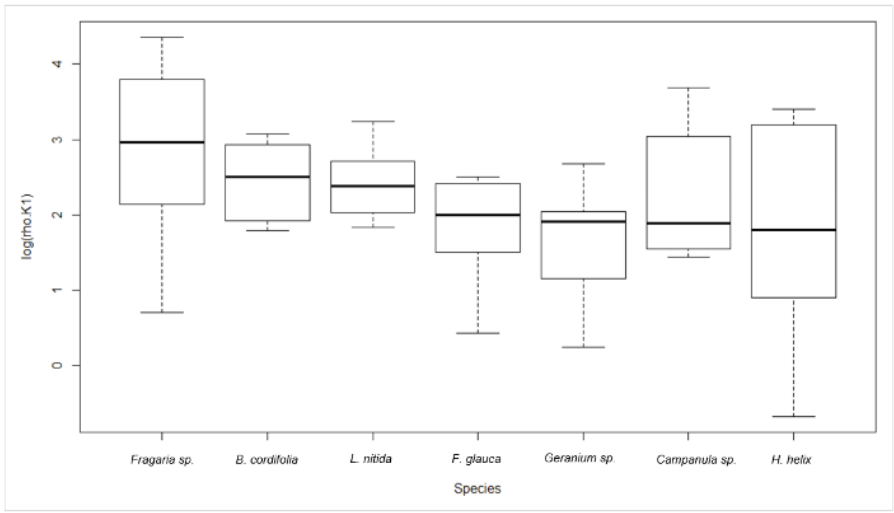

Fig. 7: Dispersion of permeability log (K) in m² (top) and Forchheimer-drag log (ρ/K_1) in kg m^{-4} (bottom) for all species, classified from high to low. For log (K) differences between species are indicated with the letters A and B.

Furthermore, Kendall rank correlation tests were performed to test the correlations between K and ρ/K_1 on one hand and PAD and porosity on the other hand and between PAD and porosity reciprocally (Fig. 8). Tau and p-values are given in Table 4. Permeability is positively correlated to porosity and negatively correlated to PAD, while for the Forchheimer-drag, the opposite is observed (as seen on the middle and bottom row, respectively). Furthermore, porosity can be seen as the best indicator (highest values of tau) for both permeability and Forchheimer-drag. In general, porosity was close to 1 for all experiments (0.956 to 0.997). Linear regression for PAD as a function of porosity for individual species showed R^2 values between 0.99 (*Campanula*) and 0.96 (*Fragaria*). For aggregation of all samples, also a strong correlation was found ($p < 2.2 \times 10^{-16}$, $R^2 = 0.85$, $\tau = -0.77$), with more scatter at higher PAD and lower porosity values. Consequentially, one linear relationship could be derived: $\varphi = 0.997 - 3.78 \times 10^{-4} \times PAD$. It appears that the Forchheimer-drag becomes more important with decreasing permeability, as evidenced by the top left figure (although the data is scattered).

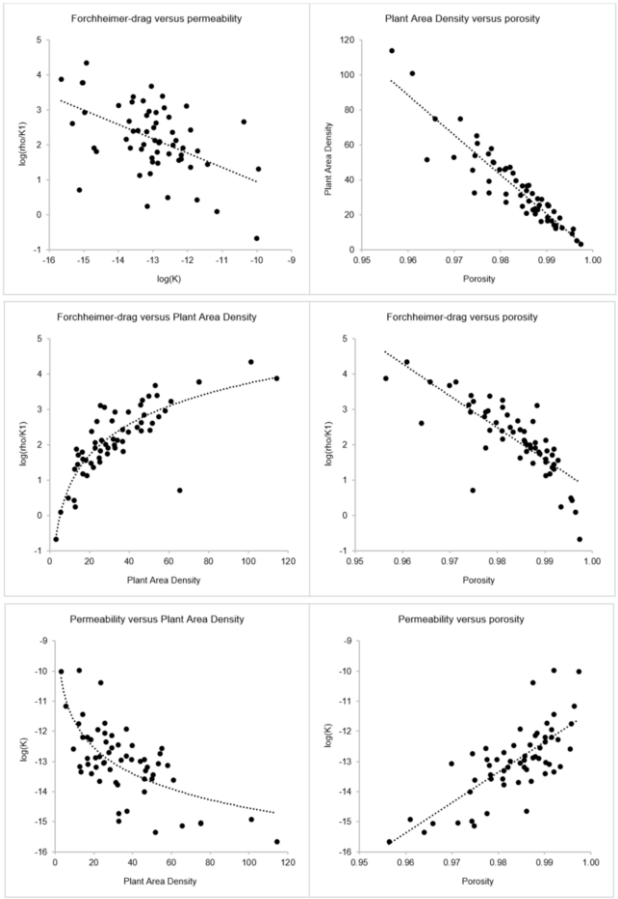

Fig. 8: Kendall rank correlations between permeability (m^2), Forchheimer-drag (kg m^{-4}), plant area density (m^2 m^{-3}) and porosity (dimensionless). Each points represents one wind tunnel run for a specific species under different wind speeds. Trendlines are also given (dotted line). The equations of the trend lines, from left to right and top to bottom, are y = -0.4107 x - 3.167, y = -2206 ln(x) - 1.6602, y = -1.248 ln(x) - 8.803, y = 101.3 x - 112.63, y = 1.2676 ln(x) - 2.0972 and y = -88.04 ln(x) + 0.7038, respectively.

Table 4: Kendall rank correlation coefficients (τ) and p-values or correlations between permeability (m^2), Forchheimer-drag ($kg.m^{-4}$), plant area density ($m^2.m^{-3}$) and porosity (dimensionless).

	Permeability (m^2)	**Forchheimer-drag (kg m^{-4})**	**PAD (m^2 m^{-3})**
Forchheimer-drag (kg m^{-4})	τ = -0.42 p-value = 1.58E-06		
PAD ($m^2.m^{-3}$)	τ = -0.43 p-value = 1.58E-06	τ = 0.65 p-value = 3.88E-13	
Porosity	τ = 0.52 p-value = 6.79E-09	τ = -0.69 p-value = 1.58E-14	τ = -0.77 p-value < 2.2E-16

3.3 Correlation between aerodynamic and morphologic parameters

For each distinct species, the morphological parameters SLA, LDI, FLS, LR, LS and LSS were analysed as a function of permeability and Forchheimer-drag. Because morphological parameters have only one value per species and permeability and Forchheimer-drag have a series of values per species, we need also one value for permeability and Forchheimer-drag to compare them with the morphological parameters. P-values obtained for the linear models are shown in Table 5. Since data was skewed, both mean and

median values of permeability and Forchheimer-drag were used. Note that LSS should be considered as a factor.

Table 5: Morphological parameters Specific Leaf Area (SLA), Lead Dissection Index (LDI), Functional Leaf Size (FLS), Leaf Ratio (LR), Leaf Size (LS) and Leaf Surface Structure (LSS) as a function of mean and median permeability (K) and Forchheimer-drag (ρ/K_1) for all species. The table shows p-values and R^2-values of the correlations as result of an ANOVA. Stars indicate significant p-values (p =< 0.05).

	Mean K	Mean ρ/K_1	Median K	Median ρ/K_1
SLA	p = 0.04* R^2 = 0.53	p = 0.17 R^2 = 0.21	p = 0.007* R^2 = 0.79	p = 0.15 R^2 = 0.23
LDI	p = 0.75 R^2 =-0.17	p = 0.73 R^2 = -0.16	p = 0.82 R^2 = -0.19	p = 0.93 R^2 = -0.20
FLS	p = 0.71 R^2 = -0.16	p = 0.018* R^2 = 0.71	p = 0.27 R^2 = 0.083	p = 0.05* R^2 = 0.47
LR	p = 0.50 R^2 = -0.088	p = 0.78 R^2 = -0.18	p = 0.62 R^2 = -0.14	p = 0.28 R^2 = 0.07
LS	p = 0.85 R^2 = -0.19	p = 0.52 R^2 = -0.09	p = 0.36 R^2 = -0.0002	p = 0.34 R^2 = 0.017
LSS	p = 0.19 R^2 = 0.34	p = 0.71 R^2 = -0.26	p = 0.10 R^2 = 0.51	p = 0.61 R^2 = -0.18

The variance of mean and especially median values of K could be explained by SLA (R^2 = 0.79) and the variance of both mean and median values of ρ/K_1 could be predicted by FLS (R^2 = 0.71). These correlations are plotted in Fig. 9. No other statistically significant correlations could be found.

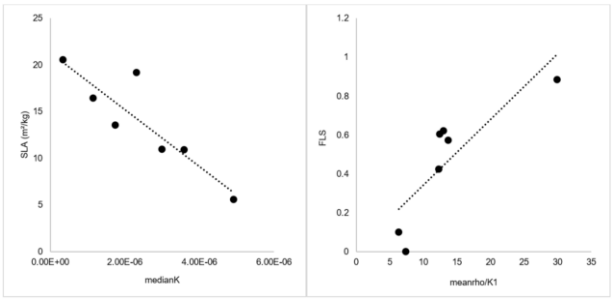

Fig. 9: Left: The correlation between SLA (m^2 kg^{-1}) and the median values for permeability K (m^2). Equation of trend line: SLA (m^2 kg^{-1}) = -(3 x 10^{-6}) median +21.323. Right: The correlation between FLS (dimensionless) and mean values for Forchheimer-drag (kg m^{-4}). Equation of trend line: FLS = 0.0338mean +0.004. Each point represents a species. Trend lines are shown as dotted lines.

3.4 Numerical modelling

Before running the CFD model, the fan curves of the duct fan, corresponding to the five power supply settings, needed to be derived. These were the boundary conditions considered in the model. Fan curves corresponding to the five power settings were derived by plotting ΔP values against the flow rate (Q) for the total number of wind tunnel runs, including all species and densities (Fig. 10). Flow rates varied from the lowest to the highest wind speed the fan could provide.

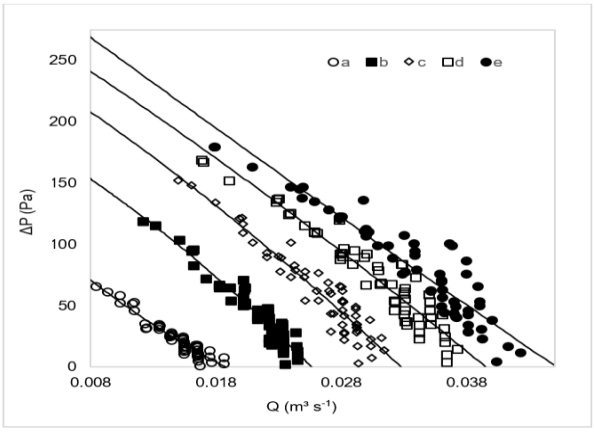

Fig. 10: Fan curve derived from the experiments with plant material in the wind tunnel, for lowest (a) to highest wind speed (e) setting. ΔP = dynamic pressure loss between before and behind the plant compartment, Q = flow rate. The full lines are the linear approximations of the fan curves, obtained

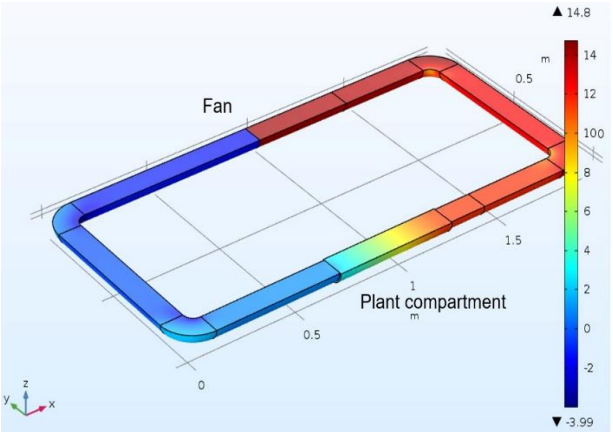

Figure 11: Typical pressure distribution obtained by the CFD model for the specific case of *Geranium* sp. (PAD = 12.64 $m^2\ m^{-3}$, φ = 0.9933, K = 1.9039 x 10^{-6} m^2, ρ/K_1 = 1.2835 kg m^{-4}, v = 1.36 m s^{-1})

A typical result obtained by the CFD model is shown in Fig. 11. The figure shows the distribution of pressure in the system for the k-ω coupled turbulence model, coupled with the Darcy-Forchheimer equation for air flow through the porous vegetation in the plant compartment. The figure clearly shows the sudden pressure drop over the fan, corresponding to the fan curve, and the gradual pressure drop over the plant compartment. Apart from the Darcy-Forchheimer model, a simple Darcy model was applied with values of K retrieved from standard Darcy's Law (Eq. 1). However, this model showed a consistent underestimation of the pressure drop compared to the experiments, because no inertial term was accounted for and porosities were high. The k-ω coupled turbulence model, which included the Forchheimer-drag for air flow through the porous vegetation section, performed best when pressure drop outcomes were correlated to experimental pressure drop results (R^2 between 0.96 and 0.98).

Model validation was performed by comparing the velocity measured with the anemometer and the velocity calculated by the model, whereby the model velocity was evaluated at the exact anemometer location (Fig. 12 left, R^2 = 0.98, NMSE = 0.016). Since the fan curve was used as a boundary condition, no velocity boundary was considered, i.e. the experimentally measured velocity was not used as a model input. Further validation of the model is evidenced by the comparison of measured and modelled ΔP values (Fig. 12 right, R^2 = 98, NMSE = 0.014). Data points tend to be more scattered at higher pressure differences (and thus wind velocities). A simple t-test showed no significant differences between model and experimental pressure drops for every separate species.

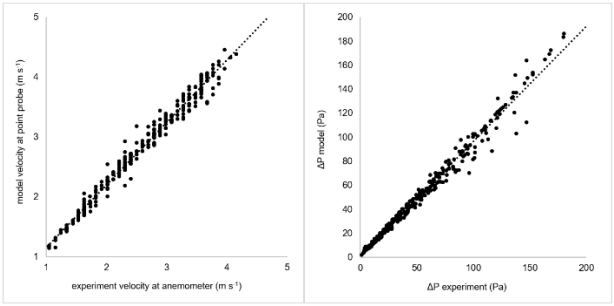

Fig. 12: Left panel: correlation between experimental and modelled wind velocities at anemometer position. Each dot represents an experimental velocity respective to its model output. Right panel: modelled versus experimental pressure drop for all species considered. Each dot represents an experimental wind tunnel run under a certain PAD of a certain species with a certain velocity, respective to its modelled counterpart. The dotted lines represent the trend line of the correlations between parameters. Respective trend line equations: y = 1.0439 x + 0.1177 and y = 0.9611 x + 0.6972.

For all species, differences between modelled and experimental normalised pressure loss were not significant. Consequentially, only modelled values are given in Fig. 13, which shows the ranking of all 7 species from low to high normalised pressure loss according to Eq. 5. A clear ranking of species can be seen, even though a normalisation for air and plant density, wind velocity and distance (length of the plant compartment) was performed. *Festuca* shows the lowest value, while *Bergenia* is on the other side of the figure, showing the largest normalized pressure loss. Moreover, an ANOVA showed a significant difference between species ($p < 2.2 \times 10^{-16}$). For every species a mean normalized pressure loss (ΔP_{norm}) was calculated for both experimental and modelled values for every species in order to test against morphological parameters. An ANOVA showed that the variance in normalised pressure loss could not be explained by either one of the considered morphological parameters.

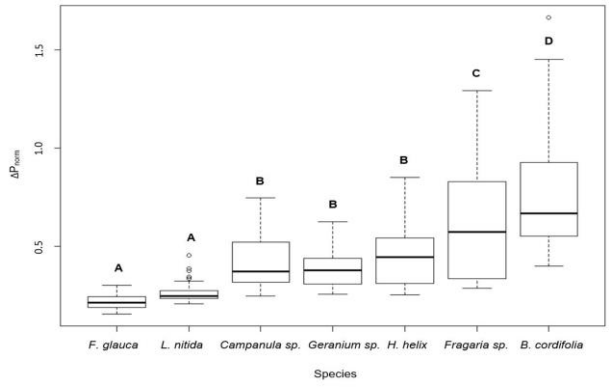

Fig. 13: Boxplots of simulated normalised pressure drop for all considered species

4 Discussion

4.1 Wind tunnel experiments

Wind tunnel experiments are a powerful way to study the aerodynamics of air flow through vegetation (e.g. K. Paul Beckett, Freer-Smith, & Taylor, 2000; Endalew et al., 2009, Gromke 2011). Relatively small and thus, cheap wind tunnels are sufficient and experiments are not too time and labour intensive. For these experiments plants were brought into a removable compartment of a wind tunnel under a range of packing densities. Compared to Lin & Khlystov, (2012a), who tested packing densities (plant volume to wind tunnel compartment volume) ranging from 0.017 to 0.040 for Pine and 0.037 to 0.055 for Juniper (both coniferous tree species), our packing density range was much wider, from 0.0018 to 0.043 (both for *Festuca*) with a median value of 0.0126 (*Lonicera*).

Regarding porosity, our values (0.9564 to 0.9973) are in agreement with the study of Buccolieri et al. (2009) who used synthetic wadding material in wire cages (φ = 0.96 - 0.975), which is assumed typical for tree crown porosities, and in agreement with Gromke et al. (2016), who used foam materials with pore volume fractions of 96.1% and 94.5%. In contrast with these studies, our research included a whole range of different porosities between and within species instead of using only one or two species with fixed porosities.

In general, most wind tunnel studies considering vegetation aerodynamics are conducted with vegetation simulators (model plants) (Buccolieri et al., 2009; Endalew et al., 2009; Gromke 2011 and references therein; Gromke et al., 2016; Wuyts et al., 2008) instead of real vegetation. The main disadvantage of using simulators is that they are artificial and rigid and thus, their structure is not affected by wind velocities, whereas the flexible structure of plants enables them to bend and even reduce drag at high wind speeds by changing their shapes. Wind tunnel experiments concerning real vegetation have mostly been used in particulate pollution capture studies (Beckett et al., 2000; Huang, Lin, Khlystov, & Katul, 2013; M.-Y. Lin & Khlystov, 2012a) but rarely in aerodynamic research, making this study innovative in terms aerodynamic research of air flow through vegetation.

4.2 Aerodynamic and morphological parameters and their correlation

Our results showed significant differences between species for permeability (Fig. 7 top) ($p = 1.63 \times 10^{-5}$), but not for the Forchheimer-drag (Fig. 7 bottom) ($p = 0.09$). This suggests that permeability is sensitive to specific differences between species, while Forchheimer-drag apparently works in a similar way regardless of species. Because permeability is dependent on porosity, pore size and detailed plant geometry (Nield, 2000), variations in means of permeability are expected to be caused by morphological and architectural differences between species. The spread of permeability values per species (see Fig. 8) can be explained by stacking convenience in the plant compartment of the wind tunnel. Species like *Hedera* and *Fragaria* could be stacked in a wider series of PAD's (thus values for PAD lying further apart, see Figure 2.3). While for species like *Geranium* and *Festuca* the variation in PAD was more limited as these species were structurally lighter and more difficult to spread homogeneously. In accordance with Sase et al. (2012), larger values of permeability were found with decreasing plant/leaf area density. However, the plants used in the experiment of Sase et al. (2012) where much further from each other, resulting in lower densities, so these values would be reported on the left side of the graph in Figure 8.

Furthermore, because of the strong correlation between PAD and porosity ($p < 2.2 \times 10^{-16}$) (Fig. 9), porosity has a strong positive correlation with permeability ($p = 0.79 \times 10^{-9}$). PAD and porosity also seem

to have a strong influence on Forchheimer-drag with p-values of 3.88×10^{-13} and 1.58×10^{-14}, respectively. This is logical as larger amounts of plant material (higher PAD, lower porosity) cause more drag and resistance to free air flow, which causes more turbulence and thus higher values for Forchheimer-drag.

Our experiments suggest that SLA can be an indicator of permeability (Table 5 and Fig. 9 left). This means that it could be possible to at least estimate the permeability of an herbaceous plant species (without a woody stem) by only assessing SLA. This makes sense, because species with large, thin and broad leaves (large SLA) cause a stronger decrease in air flow in contrast to compact, rigid leaves (small SLA), where it's easier for air flow to pass around. Even though thin leaves would bend easier, this effect seems to be subordinate. Moreover, Figure 9 (right) shows significant correlations between Forchheimer-drag and FLS. This could be explained by the leaf boundary layer, which becomes larger with increasing FLS. Thicker boundary layers signify thicker stagnant layers of air and thus an increased amount of air inertia. Please note that the correlations between SLA and permeability, and FLS and Forchheimer-drag might be subject to change. Although care was given to select representative species with a wide variety in leaf morphology, it might be that adding more species, be they shrubs or trees, would reinforce the given correlations. Therefore, still further research is needed to study these interactions.

4.3 Model vs. experiment

In recent years, CFD has become an attractive tool to predict the effects of green infrastructure on the local microclimate (heat island effect, PM deposition) and the demand for CFD studies (and appropriate parameters) for analysis of different urban planning scenarios is rising. However, CFD models can be computationally demanding, which puts limitations on this method. As a result, most CFD models represent vegetation in a rather rudimentary and theoretical way, which can simplify complex processes too much; e.g. for the assessment of PM removal capacity of vegetation, where vegetation is modelled as a simple body with theoretical leaf area densities (LAD), leading to an underestimation of PM removal capacity (Hofman et al., 2016). CFD modelling is widespread and many aerodynamic studies exist on street level (Bartzanas et al., 2002; Hong et al., 2012), but fewer work is done on vegetation level, i.e. within vegetation stands. This does not come as a surprise because detailed assessment of wind flow through vegetation is challenging. Compared to a solid body, around which the wind flow is predictable, plants are porous and flexible. Also, individual plants of the same species can have different geometries and most plants experience a shift in structure throughout the year, with as a pronounced example the seasonal leaf dynamics of deciduous species, and throughout their lifetime. The complexity of air flow through vegetation makes a simplification inevitable: in the best case, a minimum of parameters are used (here: permeability, Forchheimer-drag and porosity) in the model approach and a compromise between accuracy and computational demand needs to be found.

Figure 12b shows a strong correlation ($R^2 = 0.98$) of modelled and experimental pressure outcomes with no significant differences between modelled and experimental results for all species considered. The correlation becomes less obvious at higher pressure drop values (so also at higher wind velocities and plant densities). This can be explained by movement or compression of the vegetation in the wind tunnel at higher wind speeds, where in the model the vegetation is considered to be a static, non-moving body. Higher wind speeds cause changes in permeability due to plants being pliable. More specifically, on one hand, strong wind flow tends to bend foliage and make it more streamlined, thus increasing permeability but on the other, permeability lowers at the point where vegetation in the vegetation compartment is

blown together due to an increase in local density or porosity. Tiwary et al. (2005) suggest that grass-like and fine-leaved species appear to be more likely to be bent or compressed, while species possessing more rigid leaves and twigs are only affected by strong winds. Thus, Fig. 12b suggests that the Darcy-Forchheimer model is suitable to describe wind flow through herbaceous vegetation, with higher reliability under lower pressure drops and wind velocities. This model is a solid base for further experiments considering interactions between plants and wind-driven processes like PM deposition and heat exchange. However, it is suggested that future validation of this model should be performed with more plant functional types (e.g. shrubs and trees) with special features like very large leaves or needles, as this will contribute to the model's robustness. Furthermore, higher wind speeds should be considered to detect if the model performs also well under these conditions.

Pressure losses were normalised in order to assess differences between species. Even after normalisation for wind velocity and PAD, a measure of plant packing density, a clear difference between species was found (Fig. 13). The figure shows a ranking from small to large values for ΔP_{norm}. This is expected to be caused by species-specific morphological characteristics. However, differences in ΔP_{norm} between species could not be explained by the morphological parameters. Further research, with more species and different species traits in terms of leaf shape and size, and perhaps rigidity, should be conducted. Also no differences in mean pressure drops were found within species between modelled and experimental outcomes. This means that the model is equally able to predict pressure drop over a vegetation stand for the wide variety of species used in this research. This is promising, as living wall systems often contain a combination of different species, which points towards a broad applicability.

To describe vegetation and its aerodynamic characteristics, different measures are used in literature, which makes comparison difficult (Janhäll, 2015). Because of the setup used in our experiment it is possible that the model provided values are overestimating pressure drop in a real-life situation. This agrees with the comments of Janhäll (2015), who stated that pressure drop found in reality will be less than that found in a wind tunnel. This is because in a wind tunnel air is restricted to flowing through the vegetation whereas in reality air will partly pass around the structure due to resistance. Likewise, Tiwary et al. (2005) state that high porosity barriers are more penetrable by wind while vegetation with lower porosities forces air to pass around them.

5 Conclusions

This paper studied the interactions of vegetation and air flow and the influence of plant morphological characteristics. For the first time, several herbaceous plant species were aerodynamically characterized. A Darcy-Forchheimer model to describe air flow through the vegetation was proposed. The permeability, Forchheimer-drag and porosity of the vegetation could be used as an input for CFD-modelling. It was concluded that:

- The use of real plants instead of artificial materials is innovative in terms aerodynamic research of air flow through vegetation.
- Strong correlations between modelled and experimental data show us that the Darcy-Forchheimer model is a simple and robust way to describe air flow through vegetation, with higher reliability under lower pressure drops.
- Our results illustrate that permeability is sensitive to variation between species, while Forchheimer-drag is not.

- Because of the correlation between mean and median permeability values and SLA, it can be assumed that the differences in permeability between species can be partly explained by their SLA.
- Even though Forchheimer-drag showed no significant difference between species, mean and median values for Forchheimer-drag seem to be correlated with FLS. Therefore, we suggest FLS could be an indicator for Forchheimer-drag.
- A significant variance in normalized pressure drop exists between species, which could not be explained by the investigated morphological parameters. This suggest that more research needs to be conducted by making use of more species and other plant morphological characteristics.

It can be stated that the proposed method is useful for future modelling of vegetation and its interaction with air flow, more specifically helping investigate the process of PM deposition and thermal behaviour in green walls.

Acknowledgements

This work was supported by the VLAIO-VIS project 'Green building: green walls for sustainable buildings and cities' and the FWO-SBO project 'EcoCities: Green roofs and walls as a source for ecosystem services in future cities'.

References

Abhijith, K. V., Kumar, P., Gallagher, J., McNabola, A., Baldauf, R., Pilla, F., … Pulvirenti, B. (2017). Air pollution abatement performances of green infrastructure in open road and built-up street canyon environments – A review. *Atmospheric Environment*, *162*, 71–86. https://doi.org/10.1016/j.atmosenv.2017.05.014

Bartzanas, T., Katsoulas, N., & Kittas, C. (2012). Solar radiation distribution in screenhouses: A CFD approach. *Acta Horticulturae*, *956*, 449–456. https://doi.org/10.17660/ActaHortic.2012.956.52

Bartzanas, T., Kittas, C., & Boulard, T. (2002). Numerical simulation of the airflow and temperature patterns in a greenhouse equipped with insect-proof screen in the openings. *Acta Horticulturae*, *578*, 351–358. https://doi.org/10.1016/S0168-1699(01)00188-0

Beckett, K. P., Freer-Smith, P. H., & Taylor, G. (1998). Urban woodlands: Their role in reducing the effects of particulate pollution. *Environmental Pollution*, *99*(3), 347–360. https://doi.org/10.1016/S0269-7491(98)00016-5

Beckett, K. P., Freer-Smith, P. H., & Taylor, G. (2000). Particulate pollution capture by urban trees: Effect of species and windspeed. *Global Change Biology*, *6*(8), 995–1003. https://doi.org/10.1046/j.1365-2486.2000.00376.x

Bejan, A. (2013). Convection Heath Transfer. 4th ed. City: John Wiley & Sons, Inc., 658p., pages 537-605. Available at: http://onlinelibrary.wiley.com/book/10.1002/9781118671627.

Buccolieri, R., Gromke, C., Di Sabatino, S., & Ruck, B. (2009). Aerodynamic effects of trees on pollutant concentration in street canyons. *Science of the Total Environment*, *407*(19), 5247–5256. https://doi.org/10.1016/j.scitotenv.2009.06.016

Cameron, R. W. F., & Blanuša, T. (2016). Green infrastructure and ecosystem services - is the devil in the detail? *Annals of Botany*, *118*(3), 377–391. https://doi.org/10.1093/aob/mcw129

Castanheiro, A., Samson, R., & De Wael, K. (2016). Magnetic- and particle-based techniques to investigate metal deposition on urban green. *Science of the Total Environment*, *571*, 594–602. https://doi.org/10.1016/j.scitotenv.2016.07.026

COMSOL Multiphysics® v. 5.2. COMSOL AB, CFD Module User's Guide, Stockholm, 2017.

Connell, R. J., Endalew, a M., & Verboven, P. (2011). CFD Modelling of Kiwifruit Vines and Leaves : A method of handling multiple thin surfaces. *19th International Congress on Modeling and Simulation*, (December), 12–16.

Cornelissen, J. H. C., Lavorel, S., Garnier, E., Díaz, S., Buchmann, N., Gurvich, D. E., … Poorter, H. (2003). A handbook of protocols for standardised and easy measurements of plant functional traits worldwide. Aust. J. Bot. 51, 335-380. *Aust. J. Bot.*, *51*, 335–380. https://doi.org/10.1071/BT02124

De Maerschalck, B., Maiheu, B., Janssen, S., & Vankerkom, J. (2010). CFD-Modelling of complex plant-atmosphere interactions: direct and indirect effects on local turbulence. *HARMO 2010 - Proceedings of the 13th International Conference on Harmonisation within Atmospheric Dispersion Modelling for Regulatory Purposes*, 839–842.

Demuzere, M., Orru, K., Heidrich, O., Olazabal, E., Geneletti, D., Orru, H., … Faehnle, M. (2014). Mitigating and adapting to climate change: Multi-functional and multi-scale assessment of green urban infrastructure. *Journal of Environmental Management*, *146*, 107–115. https://doi.org/10.1016/j.jenvman.2014.07.025

Endalew, a. M., Hertog, M., Delele, M. a., Baetens, K., Persoons, T., Baelmans, M., … Verboven, P. (2009). CFD modelling and wind tunnel validation of airflow through plant canopies using 3D canopy architecture. *International Journal of Heat and Fluid Flow*, *30*(2), 356–368. https://doi.org/10.1016/j.ijheatfluidflow.2008.12.007

Gallagher, J., Baldauf, R., Fuller, C. H., Kumar, P., Gill, L. W., & McNabola, A. (2015). Passive methods for improving air quality in the built environment: A review of porous and solid barriers. *Atmospheric Environment*, *120*, 61–70. https://doi.org/10.1016/j.atmosenv.2015.08.075

Gromke, C. (2011). A vegetation modeling concept for building and environmental aerodynamics wind tunnel tests and its application in pollutant dispersion studies. *Environmental Pollution*, *159*(8–9), 2094–2099. https://doi.org/10.1016/j.envpol.2010.11.012

Gromke, C., Buccolieri, R., Di Sabatino, S., & Ruck, B. (2008). Dispersion study in a street canyon with tree planting by means of wind tunnel and numerical investigations - Evaluation of CFD data with experimental data. *Atmospheric Environment*, *42*(37), 8640–8650. https://doi.org/10.1016/j.atmosenv.2008.08.019

Gromke, C., Jamarkattel, N., & Ruck, B. (2016). Influence of roadside hedgerows on air quality in urban street canyons. *Atmospheric Environment*, *139*, 75–86. https://doi.org/10.1016/j.atmosenv.2016.05.014

Hofman, J., Bartholomeus, H., Janssen, S., Calders, K., Wuyts, K., Van Wittenberghe, S., & Samson, R. (2016). Influence of tree crown characteristics on the local PM10 distribution inside an urban street canyon in Antwerp (Belgium): A model and experimental approach. *Urban Forestry and Urban Greening*, *20*, 265–276. https://doi.org/10.1016/j.ufug.2016.09.013

Hong, B., Lin, B.-R., Wang, B., & Li, S.-H. (2012). Optimal design of vegetation in residential district with

numerical simulation and field experiment. *Journal of Central South University of Technology (English Edition)*, *19*(3), 688–695. https://doi.org/10.1007/s11771-012-1058-6

Huang, C. W., Lin, M. Y., Khlystov, A., & Katul, G. (2013). The effects of leaf area density variation on the particle collection efficiency in the size range of ultrafine particles (UFP). *Environmental Science and Technology*, *47*(20), 11607–11615. https://doi.org/10.1021/es4013849

Hunter, A. M., Williams, N. S. G., Rayner, J. P., Aye, L., Hes, D., & Livesley, S. J. (2014). Quantifying the thermal performance of green fa??ades: A critical review. *Ecological Engineering*, *63*, 102–113. https://doi.org/10.1016/j.ecoleng.2013.12.021

Janhäll, S. (2015). Review on urban vegetation and particle air pollution - Deposition and dispersion. *Atmospheric Environment*, *105*, 130–137. https://doi.org/10.1016/j.atmosenv.2015.01.052

Lin, M.-Y., & Khlystov, A. (2012). Investigation of Ultrafine Particle Deposition to Vegetation Branches in a Wind Tunnel. *Aerosol Science and Technology*, *46*(4), 465–472. https://doi.org/10.1080/02786826.2011.638346

Lin, M., Katul, G. G., & Khlystov, a. (2012). A branch scale analytical model for predicting the vegetation collection efficiency of ultrafine particles. *Atmospheric Environment*, *51*, 293–302. https://doi.org/10.1016/j.atmosenv.2012.01.004

Litschike, T., & Kuttler, W. (2008). On the reduction of urban particle concentration by vegetation - A review. *Meteorologische Zeitschrift*, *17*(3), 229–240. https://doi.org/10.1127/0941-2948/2008/0284

Madre, F., Clergeau, P., Machon, N., & Vergnes, A. (2015). Building biodiversity: Vegetated façades as habitats for spider and beetle assemblages. *Global Ecology and Conservation*, *3*, 222–233. https://doi.org/10.1016/j.gecco.2014.11.016

Mattis, S. A., Dawson, C. N., Kees, C. E., & Farthing, M. W. (2012). Numerical modeling of drag for flow through vegetated domains and porous structures. *Advances in Water Resources*, *39*, 44–59. https://doi.org/10.1016/j.advwatres.2012.01.002

Mattis, S., Dawson, C., Kees, C., & Farthing, M. (2012). Numerical Modeling of Flow Through Domains With Simple Vegetation-Like Obstacles, 1–8. Retrieved from http://cmwr2012.cee.illinois.edu/Papers/Special Sessions/Multiphase and Pore-Scale Modeling - Challenges and Perspectives/Mattis.Steven.pdf

McLellan, T., & Endler, J. A. (1998). The relative succes of some methods for measuring and describing the shape of complex objects. *Systematic Biology*, *47*(2), 264–281. https://doi.org/10.1080/106351598260914

Miguel, A. F., van de Braak, N. J., & Bot, G. P. A. (1997). Analysis of the Airflow Characteristics of Greenhouse Screening Materials. *Journal of Agricultural Engineering Research*, *67*(2), 105–112. https://doi.org/10.1006/jaer.1997.0157

Molina-Aiz, F. D., Valera, D. L., Álvarez, A. J., & Madueño, A. (2006). A Wind Tunnel Study of Airflow through Horticultural Crops: Determination of the Drag Coefficient. *Biosystems Engineering*, *93*(4), 447–457. https://doi.org/10.1016/j.biosystemseng.2006.01.016

Nield, D. A. (2000). Modelling fluid flow and heat transfer in a saturated porous medium. *Journal of Applied Mathematics and Decision Sciences*. https://doi.org/10.1155/S1173912600000122

Nowak, D. J., Crane, D. E., & Stevens, J. C. (2006). Air pollution removal by urban trees and shrubs in the United States. *Urban Forestry and Urban Greening*, *4*(3–4), 115–123.

https://doi.org/10.1016/j.ufug.2006.01.007

Ottelé, M., van Bohemen, H. D., & Fraaij, a. L. a. (2010). Quantifying the deposition of particulate matter on climber vegetation on living walls. *Ecological Engineering*, *36*(2), 154–162. https://doi.org/10.1016/j.ecoleng.2009.02.007

Perini, K., Ottelé, M., Fraaij, A. L. A., Haas, E. M., & Raiteri, R. (2011). Vertical greening systems and the effect on air flow and temperature on the building envelope. *Building and Environment*, *46*(11), 2287–2294. https://doi.org/10.1016/j.buildenv.2011.05.009

Pugh, T. a M., Mackenzie, a R., Whyatt, J. D., & Hewitt, C. N. (2012). Effectiveness of green infrastructure for improvement of air quality in urban street canyons. *Environmental Science & Technology*, *46*(14), 7692–7699. https://doi.org/10.1021/es300826w

Raupach, M. R., Woods, N., Dorr, G., Leys, J. F., & Cleugh, H. A. (2001). The entrapment of particles by windbreaks. *Atmospheric Environment*, *35*(20), 3373–3383. https://doi.org/10.1016/S1352-2310(01)00139-X

S. Sase, M. Kacira, T. Boulard, & L. Okushima. (2012). Wind Tunnel Measurement of Aerodynamic Properties of a Tomato Canopy. *Transactions of the ASABE*, *55*(5), 1921–1927. https://doi.org/10.13031/2013.42354

Tallis, M. J., Amorim, J. H., Calfapietra, C., Freer-Smith, P., Grimmond, S., & Kotthaus, S. (2015). The impacts of green infrastructure on air quality and temperature. *Handbook on Green Infrastructure*, (November), 30–49. https://doi.org/10.4337/9781783474004.00008

Tiwary, A., Morvan, H. P., & Colls, J. J. (2005). Modelling the size-dependent collection efficiency of hedgerows for ambient aerosols. *Journal of Aerosol Science*, *37*(8), 990–1015. https://doi.org/10.1016/j.jaerosci.2005.07.004

Verbruggen, S. W., Keulemans, M., van Walsem, J., Tytgat, T., Lenaerts, S., & Denys, S. (2016). CFD modeling of transient adsorption/desorption behavior in a gas phase photocatalytic fiber reactor. *Chemical Engineering Journal*, *292*(March), 42–50. https://doi.org/10.1016/j.cej.2016.02.014

Vile, D., Garnier, É., Shipley, B., Laurent, G., Navas, M. L., Roumet, C., … Wright, I. J. (2005). Specific leaf area and dry matter content estimate thickness in laminar leaves. *Annals of Botany*, *96*(6), 1129–1136. https://doi.org/10.1093/aob/mci264

White, E. V., & Gatersleben, B. (2011). Greenery on residential buildings: Does it affect preferences and perceptions of beauty? *Journal of Environmental Psychology*, *31*(1), 89–98. https://doi.org/10.1016/j.jenvp.2010.11.002

Wuyts, K., Verheyen, K., De Schrijver, A., Cornelis, W. M., & Gabriels, D. (2008). The impact of forest edge structure on longitudinal patterns of deposition, wind speed, and turbulence. *Atmospheric Environment*, *42*(37), 8651–8660. https://doi.org/10.1016/j.atmosenv.2008.08.010

The R project, https://cran.r-project.org/